

The X-HPD: Development of a large spherical hybrid photodetector

A. Braem^a, C. Joram^{a*}, J. Séguinot^a, P. Lavoute^b and L. Pierre^b

^aCERN, PH Department, Geneva, Switzerland

^bPhotonis, Brive-La-Gaillarde, France

The X-HPD concept is a modern implementation of the *Dumand* and *Lake Baikal* approach to large area photon detectors, primarily aimed at water based Cherenkov detectors. Our prototype detector consists of an almost spherical vacuum tube of 8-inch diameter with a semi-transparent bialkali photocathode and a LYSO scintillation crystal mounted in the centre of the tube. The scintillation light produced after the impact of a photoelectron which was accelerated to about 20-30 keV energy is detected by a small standard PMT. In addition to the attractive characteristics already established with its historic predecessors, namely high gain, large collection efficiency and immunity to the earth magnetic field, the X-HPD concept leads to very high effective Q.E. values, an extended viewing angle and marginal transit time spread. We present recent results obtained with a prototype tube built at CERN and a second full tube under preparation in collaboration with the company Photonis.

Submitted to Nucl. Instr. Meth. A, Proceedings of the 11th Vienna Conference of Instrumentation, 19 - 24 February 2007, Vienna, Austria.

1. Introduction

Initiated by the C2GT design study [1] we developed the concept of a large (e.g. 15-inch diameter) almost spherical Hybrid Photodetector (HPD) with centrally placed anode. While the anode was originally foreseen to consist of Silicon sensors, mounted on a ceramic cube of 15 mm side length, we chose instead a simpler and only slightly less performant alternative, namely to replace the Si-anode by a spatial scintillator crystal which is read out through a window by an external small PMT. This concept, which we call X-

HPD, is a modern implementation and extension of the *Dumand Smart PMT* [3] and *Lake Baikal Quasar* [4] approach to large area photon detectors. A similar concept, based on a hemispherical tube with readout of the scintillation light by a Geiger mode APD, is described in [5].

2. The X-HPD concept

An X-HPD consists of a glass sphere with a round opening which is sealed by a base plate. A scintillator crystal in the form of a cube or cylinder is mounted in the centre of the sphere, mechanically supported from the base plate, and

*Corresponding author, Christian.Joram@cern.ch

serves as anode. A semi-transparent photocathode covers a large part ($\approx 3/4$) of the sphere. The electrical field between cathode and anode is radial ($E \sim 1/r^2$), apart from distortions in the vicinity of the anode support. The potential difference between cathode and anode is of the order 20-30 kV. Photoelectrons bombard the scintillator and create scintillation light, which is coupled to a small photodetector. For practical reasons the photodetector is mounted outside the vacuum sphere. The price to pay are light losses at the various interfaces crystal/window/light guide/photodetector. The scintillator is coated with a reflective, metallic coating, which has the function to define an equipotential surface and to avoid scintillation light leaking out of the crystal. The symmetry of the E-field allows in principle for imaging, i.e. it can be of interest for certain applications to segment the scintillator and also the photodetector.

The main advantages of the X-HPD concept are:

- Very large viewing angle. In practice the angle is limited by the geometry of the mechanical support of the crystal and the associated E-field distortions. Values of $\pm 120^\circ$ are easily possible, corresponding to an active solid angle of 3π .
- Sensitivity increase due to 'double cathode' effect. Light which traverses the semitransparent cathode unconverted has a second chance to be detected on the opposite side.
- Low transit time spread. The central position of the anode implies that the trajectories of all photoelectrons have in first approximation the same length. The flight time differences are in the sub-ns range.

In addition, there are a number of features, which the X-HPD shares with its predecessors, the Smart and Quasar tubes:

- The scintillation mechanism leads to a first stage gain of the order of 20-40, depending on applied HV, choice of crystal and quality of light coupling. This results in a well

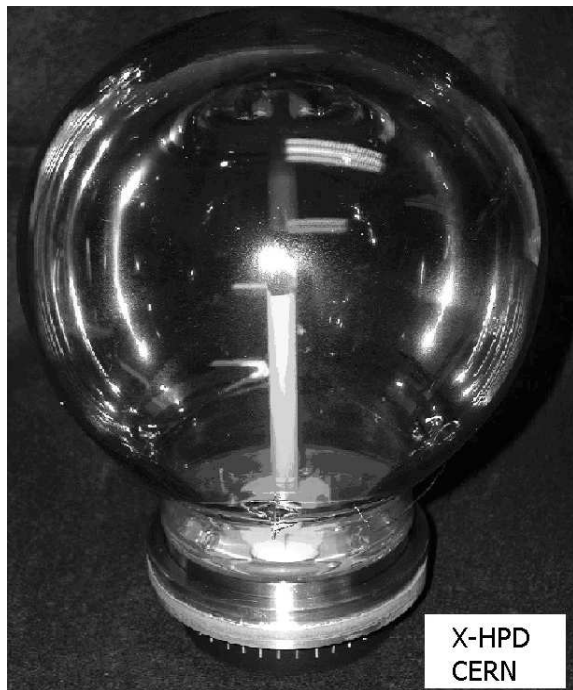


Figure 1. Photo of X-HPD prototype with metal cube anode.

defined signal, also for single photons, and a modest photon counting capability.

- The radial field geometry leads to immunity to the earth magnetic fielding and makes shielding obsolete.

3. Experimental studies

3.1. An X-HPD with metal cube anode

We fabricated in the CERN facility [6] a first X-HPD tube of 208 mm external diameter (see Fig. 1) with a cubic metal anode of 1 cm^3 volume [7]. The cube is supported in the centre of the spherical envelope by a ceramic tube fixed on the base plate of the tube. This prototype allowed to measure the QE of the bi-alkali photocathode and its variation over the full angular acceptance of $\pm 120^\circ$. For side illumination, where the light

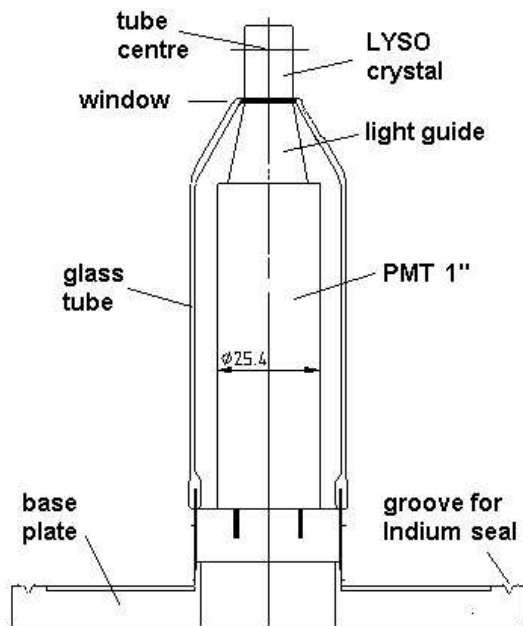


Figure 2. Simplified drawing of the X-HPD crystal anode assembly.

has a double chance to be converted, a QE of 50% was found at $\lambda = 350$ nm. In parallel a number of scintillation crystals (YAP, LSO and LYSO) of $\sim\text{cm}^3$ volume were characterized in a pumped HPD-like set-up with mono-energetic electrons of up to 29 keV energy. The electrons originate from a CsI photocathode which is exposed to light pulses from a hydrogen flash lamp. The scintillation light was coupled from the crystals through a sapphire window and detected with a standard PMT. Optical grease was used on both sides of the window. Per incident electron from the CsI photocathode up to 35 photoelectrons from the scintillator were detected.

3.2. Design and test of a LYSO based X-HPD anode

Encouraged by these results we designed a crystal anode for the first full X-HPD (see Fig. 2). We chose a cylindrical LYSO crystal of 12 mm

diameter and 18 mm length. The crystal is supported by a glass tube of 36 mm inner diameter. The tapered upper part of the tube ends with a borosilicate window on which the crystal is fixed by little dots of glue. The bottom part of the tube is attached by a glass-metal seal to the base plate which has an opening of the corresponding diameter. The side and top of the crystal are coated with a 100 nm thick Al layer, the bottom face with a MgF_2 anti-reflection coating. A light guide, made of an Al-coated truncated plexiglass cone ensures the optical contact between the window and the PMT tube of 25 mm diameter². The anode assembly was tested in the same set-up, described above, with electrons up to 27.5 keV. The photoelectric yield was found to be about 35% lower than previously measured, in good agreement with our estimate, taking into account the absence of optical grease on the vacuum side of the window. The charge spectrum, obtained by integrating the PMT signal over 150 ns, is shown in Fig. 3. The non-Gaussian part originates from electrons which are back-scattered from the crystal, depositing only a fraction of their energy. A simple Monte-Carlo, based on measured back-scattering coefficient and energy distributions of the scattered electron [8], is able to reproduce the charge spectra in good approximation. The high effective Z-value of LYSO ($Z_{eff} = 64$) leads to a back-scattering coefficient of ≈ 0.45 and favors large energy transfers to the scattered electrons with consequently reduced energy deposition in the crystal. The signal loss related to a 3σ pedestal cut was estimated to be less than 10%. Simulations with the field code SIMION 3D show that in the radial E-field of the X-HPD practically all back-scattered electrons up to 5 keV are reabsorbed in the crystal after less than 1 ns. The fate of higher energy electrons depends on scattering angles and impact point. A fraction of them will also be reabsorbed in the crystal, with delays of a few ns. Fig. 4 shows the dependence of the charge amplitude (mean of the Gaussian part) with the applied HV. The data follow approximately the expectation based on the measured relative light output of LSO [9,10]. The timing performance of

²Photonis XP3102, Gain $6 \cdot 10^6$ at 1000 V, $P/V = 2.7$

the X-HPD is driven by two effects: (1) the flight time fluctuations of the electrons between photocathode and anode and (2) the time resolution of the system LYSO / photodetector. Currently, the first effect can only be assessed by simulation. SIMION studies predict for the 208 mm tube a flight time spread of 0.4 ns (RMS) including trajectories over the complete active angular range. The second effect could be studied with our set-up employing the *first electron method*, i.e. by measuring the time between a start signal, derived from a pick-up of the flash lamp pulse and the time, when the pulse at the PMT reached the 1 p.e. level. In first approximation the timing spectrum of the first photoelectron has the form $\exp(-r_0 t)$, folded with the system time jitter, with $r_0 = N_{p.e.}/\tau_{LYSO}$ being the photoelectron emission rate. The decay time of our crystal was measured to be $\tau_{LYSO} = 45$ ns. A time spectrum measured at 27.5 kV, together with a M.C. prediction, is shown in Fig. 5. The dependence of the time resolution on the applied HV is shown in Fig. 6. The time resolution scales with the applied voltage like $1/\sqrt{U}$, i.e. like $1/\sqrt{N_{p.e.}}$, and reaches 1.7 ns at $U = 27.5$ kV.

4. Summary and outlook

The concept of the X-HPD and its attractive features have been demonstrated with a first prototype tube with metal cube anode and lab tests of a crystal anode assembly. The concept promises to beat conventional hemispherical tubes in practically all respects: sensitivity, active area, timing and signal quality. The next step, which is planned for the coming weeks is to process a tube at CERN with bi-alkali cathode and to seal the crystal anode inside the tube. The CERN facility is a transfer plant which minimizes contamination of the high field area around the anode with Potassium and Cesium from the photocathode process in order not to degrade the high voltage stability of the tube. The X-HPD will then be tested in existing infrastructure at CERN and at Photonis.

The anode configuration which we described in this article, is based on a straight forward design. We see the potential for improving the

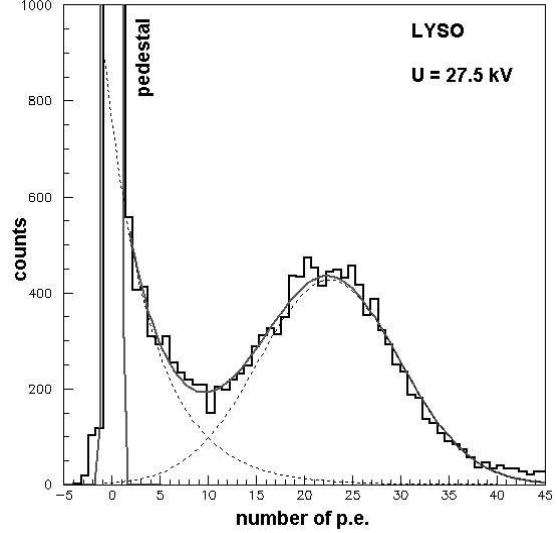


Figure 3. Charge spectrum for single photons at $U = 27.5$ kV.

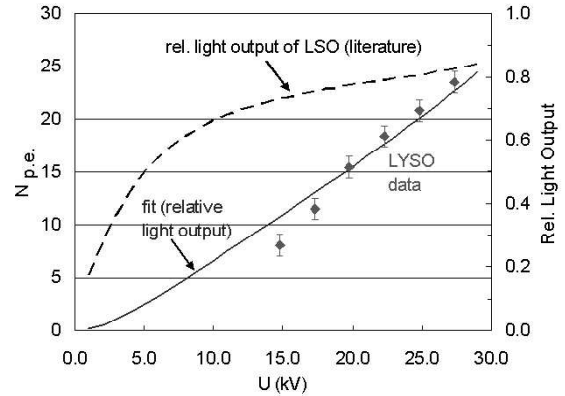


Figure 4. Charge amplitude (mean value of Gaussian part) for single photons versus applied voltage.

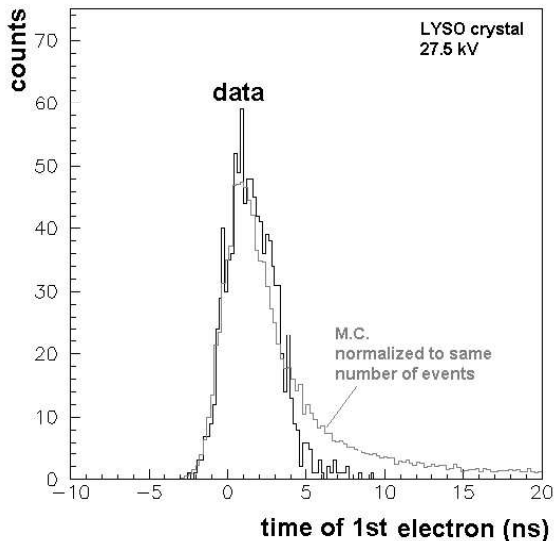


Figure 5. First electron timing. Measured and simulated time spectrum at $U = 27.5$ kV.

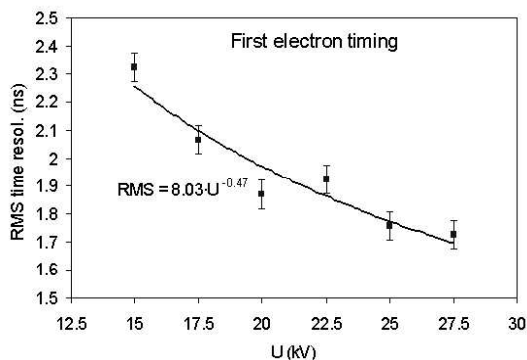


Figure 6. First electron timing. Timing resolution (RMS) versus applied voltage.

light transfer from the crystal to the photodetector which should increase photoelectric yield and consequently further improve timing and detection efficiency.

Acknowledgments

We would like to thank our technical staff at CERN, C. David, M. Delattre and M. v. Steenis, for their competent and dedicated support in preparing the HPD components and test equipment. We are grateful to G. Hallewell (CPPM Marseille) for his continuous interest and support of this project.

REFERENCES

1. A. Ball et al., *C2GT : intercepting CERN neutrinos to Gran Sasso in the Gulf of Taranto to measure θ_{13}* , Eur. Phys. J. C (2007).
2. C. Joram, *Large Area Hybrid Photodiodes*, Nucl. Phys. B. (proc. Suppl.) **78** (1999) 407-415.
3. G. van Aller et al., *A "smart" 35cm Diameter Photomultiplier*. Helvetia Physica Acta, **59**, (1986) 1119 ff.
4. R. Bagdjev et al., Nucl. Instr. Meth. **A 420** (1999) 138.
5. D. Ferenc, D. Kranich, A. Laille and E. Lorenz, *The novel Light Amplifier concept*. Nucl. Instr. Meth. **A 567** (2006) 166.
6. A. Braem, C. Joram, F. Piuz, E. Schyns and J. Seguinot, *Technology of photocathode production*, Nucl. Instr. and Meth. **A 502** (2003) 205.
7. A. Braem et al., Nucl. Instr. Meth. **A 570** (2007) 467.
8. E.H. Darlington, *Backscattering of 10-100 keV electrons from thick targets*, J. Phys. D, Vol. 8, (1975) 85-93
9. W. Mengesha et al., IEEE Trans. Nucl. Sci. Vol. **45**, No. 3 (1998) 456
10. W.W. Moses, Current trends in scintillator detectors and materials, Nucl. Instr. Meth. **A 487** (2002) 123-128